THE JOURNAL OF PHYSICAL CHEMISTRY B

Article

pubs.acs.org/JPCB

Quantum Mechanical Interpretation of Intermolecular Vibrational Modes of Crystalline Poly-(*R*)-3-Hydroxybutyrate Observed in Low-Frequency Raman and Terahertz Spectra

Shigeki Yamamoto,*[,†] Yusuke Morisawa,[‡] Harumi Sato,[†] Hiromichi Hoshina,[§] and Yukihiro Ozaki*[,†]

[†]Department of Chemistry, School of Science and Technology, and Research Center for Environment Friendly Polymers, Kwansei Gakuin University, Gakuen 2-1, Sanda, Hyogo 669-1337, Japan

[‡]Department of Chemistry, School of Science and Engineering, Kinki University, 3-4-1 Kowakae, Higashiosaka City, Osaka 577-8502, Japan

[§]RIKEN, 519-1399 Aramaki-Aoba, Aoba-ku, Sendai, Miyagi 980-0845, Japan

Supporting Information

ABSTRACT: Low-frequency vibrational bands observed in the Raman and terahertz (THz) spectra in the region of 50−150 cm^{-1} of crystalline powder poly-(*R*)-3-hydroxybutyrate (PHB) were assigned based on comparisons of the Raman and THz spectra, polarization directions of THz absorption spectra, and their congruities to quantum mechanically (QM) calculated spectra. This combination, Raman and THz spectroscopies and the QM simulations, has been rarely adopted in spite of its potential of reliable assignments of the vibrational bands. The QM simulation of a spectrum has already been popular in vibrational spectroscopies, but for low-frequency bands of polymers it is still a difficult task due to its large scales of systems and a fact that interactions among polymer chains should be considered in the calculation. In this study, the spectral calculations with the aid of the Cartesian-coordinate tensor transfer (CCT) method were applied successfully to the crystalline PHB, which include the explicit consideration of an intermolecular interaction among helical polymer chains. The agreements between the calculations and the experiments are good in both the Raman and THz spectra in terms of spectral shapes, frequencies, and intensities. A Raman active band at 79 cm^{-1} was assigned to the intermolecular vibrational mode of the out-of-plane C═O + CH_3 vibration. A polarization state of the corresponding far-infrared absorption band at ∼82 cm^{-1}, perpendicular to the helix-elongation direction of PHB, was reproduced only under the explicit correction, which indicates that this polarized band originates from the interaction among the polymer chains. The calculation explored that the polarization direction of this band was along the *a* axis, which is consistent with the direction in which weak intermolecular hydrogen bonds are suggested between the C═O and CH_3 groups of two parallel polymer chains. The results obtained here have confirmed sensitivity of the low-frequency vibrational bands to the weak hydrogen bonds among the polymer chains.

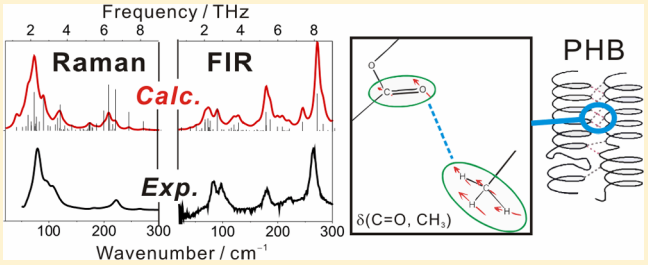

INTRODUCTION

Vibrational bands of molecules in a low-frequency region, typically below ∼300 cm^{-1}, arise not only from intramolecular interactions but also from intermolecular interactions of the molecules. Vibrational spectroscopy in this frequency region has focused on higher order structures of proteins,[1−5] intermolecular interactions, and dynamics of small molecules in condensed phases.[6−13] Polymers are also tempting targets for low-frequency vibrational spectroscopy because the spectra can directly provide information about noncovalent bonds among polymer chains, which are keys to understand properties of polymers, and various polymers have been subjected to FIR and Raman measurements since the 1950s.[14−17] Although spectrum interpretation for polymers is not straightforward, they provide valuable information about interactions and dynamics of polymers which can influence on their higher order structures. It has been proposed that vibrational modes observed in the 50−250 cm^{-1} region reflect hydrogen bonds themselves, with the majority observed in the 100−180 cm^{-1} region.[6,17−19] For small molecules, for example, the vibrational mode at 105 cm^{-1} of 7-azaindole dimer was assigned to the intermolecular stretching mode of the dimer.[6] In the case of polymer, for instance, it was suggested that a FIR absorption band at 105 cm^{-1} of crystalline polyurethane can be assigned to the interchain hydrogen bonds between NH and C═O groups, but it is not so clear.[17] Thus, sure assignments of the low-frequency bands of polymers have been desired to understand their interactions in crystal growth, aggregation, and formation of higher-order structures. In this study, we have targeted a biodegradable polymer, poly-(*R*)-3-hydroxybutyrate (PHB), to

Received: September 30, 2012
Revised: January 15, 2013
Published: January 22, 2013

   dx.doi.org/10.1021/jp309704k | *J. Phys. Chem. B* 2013, 117, 2180−2187

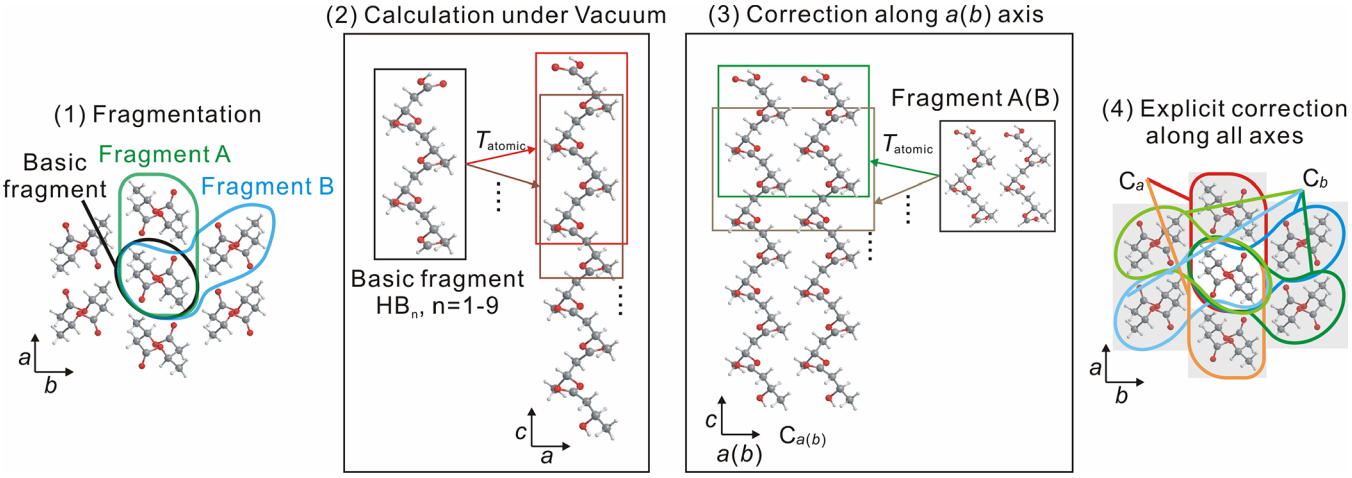

Figure 1. Schematic presentation of the Cartesian coordinate tensor transfer as applied to the crystalline polymer PHB. (1) Fragmentations of the molecule; molecular fragments are created from the X-ray crystal structure of PHB.[24] Basic fragment contained one isolated polymer chain. Fragments A and B comprised two chains along the *a* axis and the *b* axis, respectively. (2) Calculation under vacuum. Calculated atomic tensors of the basic fragment with length of *n* (*n* = 1−9) monomer unit are transferred back to the polymer chain. (3) Interchain interactions along *a* (or *b*) axis are taken into account by transferring calculated tensors of the fragment A(B) and averaging with those of the vacuum calculation. Fragment A or B contains two chains with a length of three monomer units. Fragments with resultant tensors (C_a and C_b) are utilized in the next step. (4) Calculation under explicit correction. Tensors of both of the fragment C_a and C_b are transferred to consider intermolecular interactions along the all axes of the PHB. End effects are also canceled by overlapping the fragments.

assign its FIR bands by comparing them with Raman bands, quantum mechanical calculations of the spectrum, and their polarization measurements. The intermolecular interactions among the polymer chains are considered explicitly in our quantum mechanical calculations, which have been waiting for realistic simulations of the low-frequency bands.[20,21] At the same time, the experimental low-frequency Raman spectrum of PHB is compared with the calculated Raman spectrum in order to ensure the assignments. The comparisons of these complementary spectroscopic methods, terahertz (THz) absorption and low-frequency Raman, combined with the spectral simulations will enable the certain assignments of the low-frequency vibrational bands.

PHB is produced by universal natural bacteria, and has been attracting keen interest because of its good thermal and mechanical properties.[22,23] It is known that PHB takes a lamellar helical structure in its crystal form.[24,25] Based on detailed studies by wide-angle X-ray diffraction, IR and Raman spectroscopies, differential calorimetry, and computer simulations of model molecules, it becomes clear that weak intermolecular hydrogen bonds exist among the CH_3 and O═C groups of PHB and that they play a critical role in the crystal formation of PHB.[26−30] Weak hydrogen bonds between C−H and C═O groups have been studied mainly in the systems of small molecules,[31−34] but rarely found in high polymers. Their bonding energies are weak (around 5 kJ/mol[28,30,32,34]); however, these interactions can be a dominant one between polymer chains in condensed phases. This directional weak interaction can determine the folding direction of the crystalline PHB.[26] Therefore, it is meaningful to study the weak intermolecular hydrogen bonds of PHB for understanding the nature of its folding to higher order structures.

Owing to the recent development of terahertz time-domain spectroscopy (THz-TDS), rapid and easy data acquisition has become possible of low-frequency vibrational bands. THz spectra of some polymers have been measured by THz-TDS and the observed spectra yielded information about their higher order structure and dynamics.[21,35−39] In our previous studies, THz spectra of PHB were measured by THz-TDS and Fourier transform FIR spectroscopy. The temperature- and polarization-dependent spectra of PHB indicated that the low-frequency vibrational bands can reflect the weak intermolecular hydrogen bonds between the CH_3 and O═C groups.[35,36] The lamellar crystalline form of PHB showed THz absorption peaks in the region of 70−120 cm^{-1} (~2.1 to ~3.6 THz), which were not observed in the amorphous state of PHB. The polarization spectra showed clear anisotropies of vibrational peaks. A band at ~80 cm^{-1} was perpendicularly polarized to the helical axis (*c* axis in Figure 1) of PHB, suggesting its origin in the intermolecular hydrogen bonds among the PHB chains. However, the assignment of those vibrational modes contains some uncertainties if only based on the experiments; spectral simulations based on theories are required.[20,21] However, the precise calculation with high level of theory requires long or unrealistic calculation time for big molecules such as polymers. In addition, it is also a difficult task to consider noncovalent bonds in the spectral calculations owing to numerical instability in the optimization process[40] and swelled scales of the system. As far as we know, there is no quantum mechanical simulation of low-frequency vibrational bands of polymers with considering interchain interactions.[20,21]

The Cartesian coordinate tensor transfer (CCT) method[41,42] can be applied for the calculation of the vibrational spectrum of big molecular system with a reasonable time, while with a nearly ab initio quality. By using the CCT method, we can easily parallelize the calculation by fractionating a big molecular system to smaller molecular fragments. This method enables the calculation of tensors of intermolecular fragments separately from those of intramolecular fragments,[43,44] which accelerates the calculation speed and clarifies the spectral contributions from the intra- and the intermolecular interactions. This method has been successfully applied to the higher-frequency vibrational bands of large molecules such as polypeptides,[42,45−49] protein,[44] and nucleic acids,[43,50−52] but not yet to the low-frequency bands below 100 cm^{-1}. In this paper we

dx.doi.org/10.1021/jp309704k | J. Phys. Chem. B 2013, 117, 2180−2187

applied this method to the PHB system in order to consider the intermolecular interactions explicitly. In the CCT method, an original big molecular system is cut into smaller fragments, and their property tensors (force field, Raman polarizability, dipole derivative, etc.) are calculated at a high level of theory and then transferred back to the original molecular system atom by atom. The neighbor fragments should contain the overlapped regions in their structures to maintain the continuity of the tensors in the big molecular system by weighted-averaging the tensors in the overlapped regions. The structures of fragments are optimized in the normal mode coordinate,[40,53] which provides the smallest geometrical deviations from the original structure while with relaxing the interested vibrational bands. It is frequently observed that the fully relaxed optimization in redundant/internal coordinate of the molecular fragments results in large deviations from realistic polymer geometries (for example, a model system of nylon[54]). The partial optimization in internal coordinate with fixing the distances or angles may be done; however, we cannot know a priori which geometrical parameters influence the vibrations. Thus, it is dangerous for the low-frequency region where the vibrations can contain rotations and translations of local parts of molecular system. In the partial optimization in normal mode coordinate, uninterested lower frequency vibrations were fixed, and interested higher vibrations were relaxed. In the previous studies, the vibrations below 300 cm^{-1} were fixed with relaxing the higher frequency vibrations.[42−52] For the calculation of the spectra in the THz region, the very low vibrations should be fixed (for example, below 20 cm^{-1} in this study) in order to relax the vibrations higher than the fixed frequency. This quantum mechanical calculation aided by CCT method will open a new avenue for exploring intermolecular interactions of polymers, including weak hydrogen bonds, which appeared in the vibrational spectra.

MATERIALS AND METHODS

Materials and Spectral Measurements. The crystalline powder of poly-(*R*)-3-hydroxybutyrate (PHB, Aldrich) was used as received. Raman spectra of the PHB were measured at room temperature by using a Raman microscope (HR800, Horiba) with a laser excitation at 514.5 nm (stabilite 2017, Spectra-Physics). The laser power used was 16 mW at the sample position. The Raman scattered light was collected by an objective lens (50×), passed through an edge-filter with a wavenumber cutoff at ∼50 cm^{-1}, diffracted by a grating of 1800 lines/mm, and then detected by a Peltier-cooled CCD. The total exposure time was 500 s. Infrared spectrum of crystalline PHB shown in this paper was taken from a previous paper.[36]

Spectra Calculations. The initial structure of the lamellar crystalline PHB was reconstructed based on the geometry determined by X-ray crystallography.[24] From this structure, molecular fragments containing *n* number of monomer units were created along the polymer chain (basic fragment) (Figure 1). Additional fragments containing two polymer chains (each chain contained 3 monomer units) were created along the *a* axis (fragment A) and the *b* axis (fragment B) in order to take into account the intermolecular interactions among the chains. The fragments were partially optimized in the normal mode coordinate[40] with fixing the vibrational modes between *i*20 and 20 cm^{-1} (*i* means imaginary frequency). By this procedure, the higher frequency modes above 20 cm^{-1} can be relaxed with a small structural deviation from the initial structure. The normal mode optimization was performed by using QGRAD program[55] combined with the Gaussian 09[56] at the level of B97-1[57]/6-31++G**. The B97-1 functional was used as default because of its superior performance on hydrogen bonds compared to conventional functionals such as B3LYP.[58] The other functionals were also tested. Harmonic force field, derivatives of electric dipole polarizabilities, and the dipole derivatives were calculated for the fragments at the same level as the optimization. For the calculation under vacuum, the only tensors of the basic fragment were transferred back to the whole structure of PHB by using a CCT program.[41,42] In the calculation under explicit correction of intermolecular interactions, the tensors of the fragment A and fragment B were also transferred and averaged with those of the vacuum calculation. The Raman and IR absorption spectra were generated with a Lorentzian function with Boltzmann temperature correction, $I/\omega_i[1 - \exp(-\omega_i/(kT))]^{-1}\,[4((\omega - \omega_i)/\Delta) + 1]^{-1}$, where ω_i is the vibrational frequency, k is the Boltzmann constant, T is temperature of 295 K, and Δ is full width at half-maximum of 10 cm^{-1}. Normal mode analysis was done with the PLAY program.[59]

RESULTS AND DISCUSSION

Figure 2 shows an experimental Raman spectrum of the crystalline powder PHB in the 50−3200 cm^{-1} region. Of note

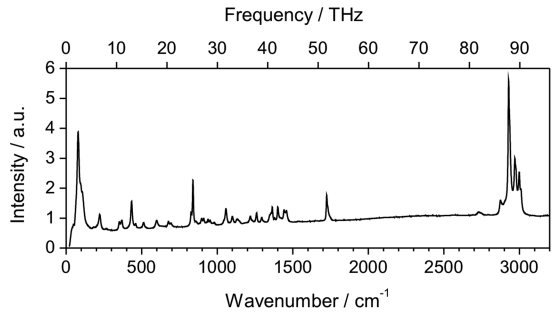

Figure 2. A Raman spectrum of crystalline powder of PHB measured at room temperature. Laser power at the sample 16 mW, exposure time 500 s.

is that a strong Raman band is observed in the low frequency of ∼80 cm^{-1} in the spectrum (Figure 2), the intensity of which is comparable to those of the C−H stretching vibrations. This band is a Raman-active band, as the THz absorption spectra showed a relatively weak peak in the same region (Figure 4, right, bottom). Three strong Raman peaks are observed at 79, 98, and 107 cm^{-1}, and their counterparts are found also in a FIR spectrum of PHB.[36] At first we checked the influence of the optimization methods on the optimized geometry of a short single chain of PHB and its calculated spectra. Figure 3 compares the structure of PHB with six monomer units in the crystal (left), optimized in the normal mode (center), and in full optimization (right). It can be seen that the full optimization caused the large structural deviations at the chain ends; however, in the normal mode optimization, the deviation is much smaller and geometry is closer to the crystal structure. The small geometrical deviations found in the normal mode optimization should originate from relaxation of the molecular vibrations higher than the fixed frequency, 20 cm^{-1}. The calculated Raman and FIR spectra based on these optimized geometries are shown in Figure S1 in the Supporting Information. They indicate some similarities between the two optimization methods especially at the higher frequency region

dx.doi.org/10.1021/jp309704k | J. Phys. Chem. B 2013, 117, 2180−2187

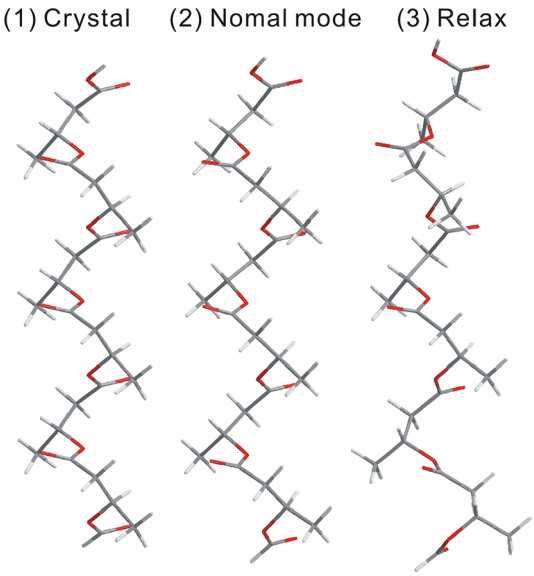

Figure 3. Comparisons of molecular geometry of single isolated PHB chain with six monomer units (1) found in the PHB crystal,[24] (2) optimized in the normal mode coordinate with fixed vibtational modes below 20 cm^{-1}, and (3) fully optimized geometry. Both of the calculations were done in vacuo at the level of B97-1/6-31++G**.

over 1200 cm^{-1}; however, the full optimization gives many fine peaks and peak splits at the lower frequency region, which should be due to the geometrical deviations of the chain ends as seen in Figure 3. Influence of the fixed vibrational modes on the higher relaxed modes can be examined for the fragment with one monomer unit of PHB where the optimized geometry in the normal mode is very similar to the fully relaxed structure (Figure S2 in the Supporting Information). In this case, the normal optimization with fixing below 20 cm^{-1} gave the similar spectra to those in fully relaxed optimization in the region higher than around 40 cm^{-1}. Thus, this optimization method can be applied to the low-frequency vibrations higher than 40 cm^{-1}. We want to emphasize again that the full optimization cannot be applied to the intermolecular fragments (Figures 1−3), because of its numerical instability and large deviations of the resultant geometries from the crystal structure. On the basis of these results, we selected the normal mode optimization for the calculations of PHB in order to include the interactions among polymer chains in the quantum mechanical calculation scheme.

Parts A and B of Figure 4 compare the calculated (top and middle) and the experimental (bottom) Raman and FIR spectra of crystalline PHB. The calculations were carried out under vacuum (top) and with the explicit correction for the intermolecular interactions (middle). In these calculations, a basic fragment with 9 monomer units was used, which can cover all covalently bonded parts of PHB in the lamellar system (the helix length of lamellar PHB is reported as about 8 to 9 monomer units[60]). The main features in the Raman and FIR spectra of PHB were reproduced by both calculations irrespective of the intermolecular interactions were considered or not. However, note that the explicit correction improved significantly the agreements between the experiments and the calculations in terms of the spectral shapes, relative intensities, and relative frequencies. For example, the band shapes of the Raman bands in the 50−100 cm^{-1} region become much closer to the experimental results upon considering the intermolecular corrections. The corresponding FIR features also show the similar tendency; broad IR bands at 74 and 82 cm^{-1} in the vacuo calculation split into two bands at ∼73 and 90 cm^{-1} in the explicit calculation, becoming closer to the experimental ones. The better agreements observed in the explicit calculations suggest a delicate but significant influence of the intermolecular interactions on these lower frequency vibrations. The good agreements between the explicit calculations and the experiments in both of the Raman and FIR spectra enable the assignments of these bands, as the experimental Raman bands at 79 and 98 cm^{-1} correspond to those at 73 (out-of-plane C═O + CH_3) and 90 (CH_2 + CH_3) cm^{-1} in the explicit calculation. The frequency difference of these two peaks is 17 cm^{-1} in the calculation; it agrees well with the experimental

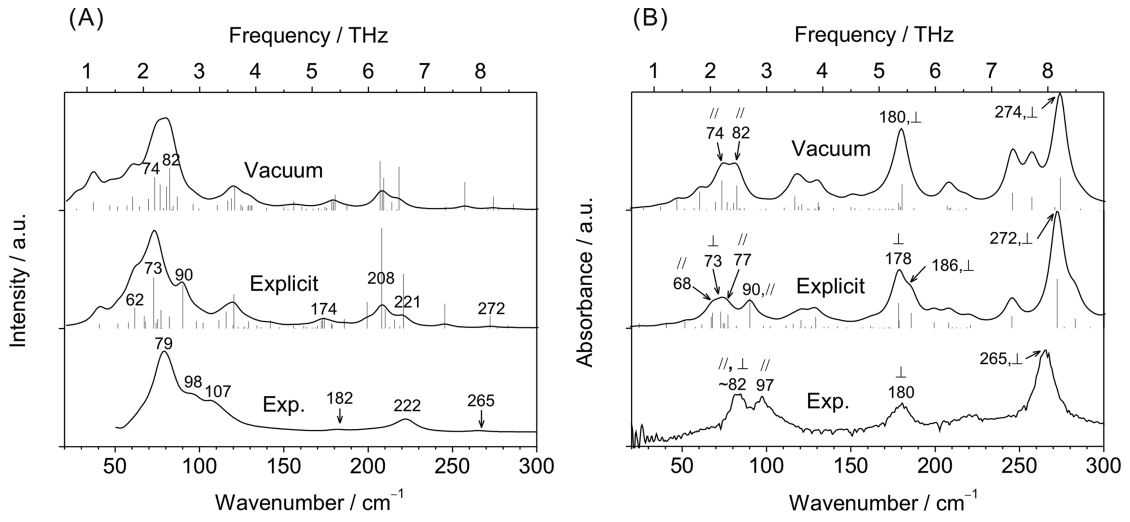

Figure 4. Comparison of the calculated (top and middle) and experimental (bottom) Raman (A) and FIR absorption (B) spectra of crystalline PHB. The calculations were carried out under vacuum (top) and with the explicit correction for the intermolecular interactions (middle). A basic fragment with nine monomer units was used in these calculations. The polarization states of the IR absorption bands are also indicated as parallel (∥) or perpendicular (⊥) to the *c* axis of the PHB based on the THz-TD spectroscopy (note that the experimental band at around 82 cm^{-1} is depolarized with respect to the *c* axis).[35] The experimental FIR spectrum was taken from ref 36

dx.doi.org/10.1021/jp309704k | J. Phys. Chem. B 2013, 117, 2180−2187

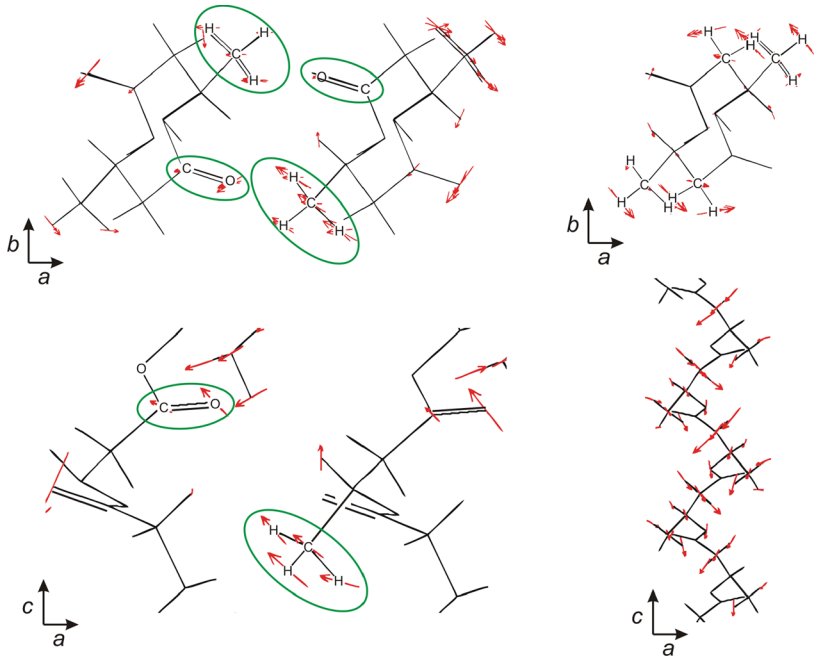

Figure 5. Calculated atomic motions of the vibrational modes of the lamellar crystalline PHB: (left) the out-of-plane C═O + CH_3 at 73 cm^{-1} and (right) CH_2 + CH_3 at 90 cm^{-1} under the explicit correction.

Table 1. Assignments of Raman and FIR Bands Based on Two Kinds of Calculations and Polarization States of FIR Absorption Bands

experiments			calculations			
Raman, RT	FIR,[a] RT	FIR,[b] 10 K	vacuum		explicit	
79	82(∥,⊥)[c]	85(∥)	74(∥)	CH_2 + CH_3	68(∥)	COO + CH_2 + CH_3
		94(⊥)			73(⊥,*a*)	C═O(o.p.) + CH_3
					77(∥)	COO + CH_2 + CH_3
98	97(∥)	98(∥)	83(∥)	C═O(o.p.) + CH_3	90(∥)	CH_2 + CH_3
107		114(∥)				
182	180(⊥)	169(⊥)	180(⊥,*b*)	CH_2 + CH_3	178(⊥,*b*)	CH_2 + CH_3
		178(⊥)			186(⊥,*b*)	
222		226(∥)				
265	265(⊥)	266(⊥)	274 (⊥,*b*)	OCH_α + CH_3	272(⊥,*b*)	OCH_α + CH_3

[a]Frequencies based on ref 36 and polarization states based on ref 35. [b]Based on ref 36. [c]FIR polarization state against the *c* axis of PHB. The polarization states of the FIR absorption bands are indicated as parallel (∥) or perpendicular (⊥) to the *c* axis of the PHB (note that the experimental FIR band at 82 cm^{-1} at room temperature is depolarized with respect to the *c* axis). The main polarization directions of the perpendicularly polarized bands are shown as *a* or *b*, which means along the *a* or *b* axis of PHB. RT = room temperature, o.p. = out of plane.

difference, 19 cm^{-1}. The broad experimental FIR band at ~82 cm^{-1} would correspond to the overlap of three calculated peaks at 68, 73, and 77 cm^{-1}. The atomic motions of the modes of out-of-plane C═O + CH_3 and CH_2 + CH_3 are shown in Figure 5.

In order to confirm the assignments based on the spectral shape similarities discussed above, the polarization directions of the IR peaks are compared among the calculations and the polarized THz spectra (Figure 4, Table 1).[35,36] In the experiment at room temperature, the higher-frequency peak at 97 cm^{-1} is polarized parallel to the *c* axis of the PHB, and the lower band at ~83 cm^{-1} is depolarized with respect to the *c* axis. At 20 K, the lower depolarized band is split to two bands, polarized parallel (85 cm^{-1}) and perpendicular (94 cm^{-1}) to the *c* axis. The explicit calculation shows good agreements in the polarization states in the whole THz spectral range, but the vacuo calculation cannot reproduce the experimentally observed perpendicular component at ~82 cm^{-1} (Figure 4 and Table 1). Therefore, this perpendicular component originates from the intermolecular interactions among the PHB chains. Furthermore, this band is assigned to the out-of-plane C═O + CH_3 vibration, and its polarization direction is explored to be along the *a* axis of PHB. Therefore, we can conclude that the intermolecular interactions on the C═O and CH_3 groups are directional as working along the *a* axis of the PHB. Our previous studies have suggested, based on the results of wide-angle X-ray diffraction and IR spectra of PHB and quantum mechanical calculation for model molecules, that the weak intermolecular hydrogen bonds exist along the *a* axis of PHB between the C═O and CH_3 groups of different polymer chains.[26−30] The THz spectroscopy study has also proposed that the low-frequency bands between 70 and 120 cm^{-1} are related to the weak intermolecular hydrogen bonds.[36] The present low-frequency Raman and FIR results are fully consistent with them, and strongly support their suggestions. From these facts discussed above, we conclude that the band

dx.doi.org/10.1021/jp309704k | J. Phys. Chem. B 2013, 117, 2180−2187

observed at 79 cm^{-1} is sensitive to the weak hydrogen bonds among the PHB chains along the *a* axis. Previous FIR studies indicated that the stretching modes of the hydrogen bonds usually appear in the region of 100−180 cm^{-1};[18] for example, a band due to a hydrogen bond between the C═O and NH groups of polyurethane appeared at 105 cm^{-1}.[17] The frequency of the hydrogen-bonding mode observed at 79 cm^{-1} of the PHB is lower than that of the hydrogen bond of the polyurethane by 26 cm^{-1}. This unusually low vibrational energy may be explained by the weakness of the hydrogen bonds via C═O and H−C groups in PHB.

It can be seen in Table 1 that the relative frequencies of the vibrational modes are dependent on whether or not the intermolecular interactions are included in the calculations. In the vacuo calculation, the two calculated peaks at 74 and 83 cm^{-1} correspond to a vibrational mode of CH_2 + CH_3 and that of out-of-plane C═O + CH_3, respectively. However, in the intermolecular-corrected calculation, the relative frequency of these bands is inverted as the peaks appeared at 90 and 73 cm^{-1}, respectively. This result indicates the force constants of these vibrational modes are strongly dependent on the intermolecular interactions among C═O, CH_3, and CH_2 groups.

As seen above, the weak interactions among polymer chains are well reproduced by the explicit calculation, although only the interactions between two chains are considered in the DFT calculations of the property tensors. It suggests that the weak interactions between the C═O and CH_3 groups nearly complete in the two adjacent polymer chains and do not influence on the next third polymer chains. The potential of weak hydrogen bonds would be consumed rapidly by the bond pairs in the condensed phase. Further improvement of the calculation may be possible by considering the more distant molecular fragments; however, the optimization with the larger intermolecular fragments, for example, three chains along the *a* axis of PHB, failed in our calculation scheme, probably due to numerical instability in the optimization process because of weakness of the interactions considered and higher degree of freedom of motion in the system compared to the fragment with two chains.

There are some residual mismatches between the experiments and the explicit calculations in terms of vibrational frequencies and intensities. For example, the calculated Raman and FIR bands around 120 cm^{-1} are difficult to be assigned to the experimental band. That might correspond to the experimental Raman band at 107 cm^{-1}, but not clear. Deviations could be originating from fluctuations of the PHB structure from the crystal one, under- or overestimation of the weak interactions in the DFT calculations, or anharmonicity of the vibrational modes, but they are beyond our goal in this paper. The anharmonicities of molecular vibrations have been believed as an important factor in the low-frequency region because of their nature with shallow potentials. The consideration of them might improve the agreements in the future. Our calculations demonstrate the importance of the explicit correction for the intermolecular interactions in simulations of low-frequency vibrational spectra in condensed phases.

Dependences of the calculated Raman and FIR absorption spectra on the DFT functional are shown in Figure 6. Similar spectral profiles were obtained for all functionals (B3LYP,[61] B3PW91,[62] B97-1,[57] X3LYP,[63] B97D,[64] CAM-B3LYP[65]). There is no big difference in the spectra among the functionals;

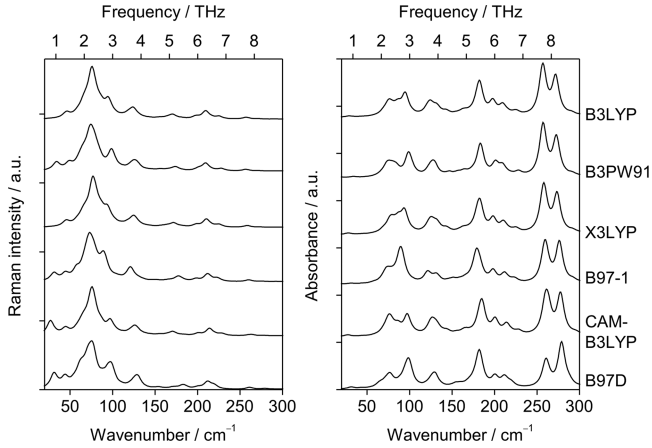

Figure 6. Dependence of the calculated Raman (left) and FIR absorption (right) spectra of crystalline PHB on the functional with the 6-31++G** basis set. The calculations were done with the basic fragment with six monomer units and the intermolecular fragment A.

our assignments based on the calculations with B97-1 functional are not affected by the functional adopted. In our case, dispersion-corrected newer functionals (B97D and CAM-B3LYP) show similar results with the other functionals. The spectral shapes of the FIR spectra below 100 cm^{-1} are relatively sensitive to the functionals if compared to the higher frequency region.

Delocalized nature of the vibrations in one polymer chain can be observed in the vacuo calculations with different lengths of the basic fragment (Figure 7). As seen, the main spectral

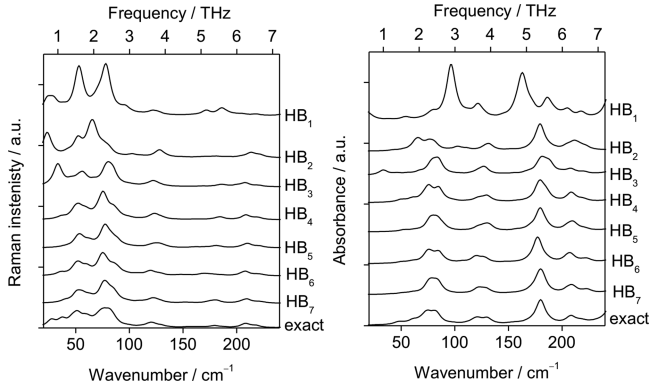

Figure 7. Dependence of the calculated Raman (left) and FIR absorption (right) spectra of crystalline PHB on the length of the basic fragment used in the tensor transfer. The calculated property tensors of the fragment HB_n (*n*, number of monomer units in the basic fragment) were transferred to the HB_9 chain. The calculations were done in vacuo.

patterns are converged for calculations with fragment of over 4 monomer units. However, the fine structures of the bands are depending on the chain length even over 4 monomer units, especially in the region below 100 cm^{-1}. For precise calculations of spectra in the THz region, it will be necessary to use a basic fragment which has a similar length to the real system. In the case of PHB, the helix length is about 8 to 9 monomer units,[60] which is consistent with our calculation condition adopted in Figure 4.

The QM calculation aided by the CCT method for the low-frequency vibrational spectra of polymers has some advantages

dx.doi.org/10.1021/jp309704k | J. Phys. Chem. B 2013, 117, 2180−2187

over the former calculation methods of which applications are actually limited to isolated polymer chains only. The first point is the CCT enables the explicit considerations of the weak noncovalent bonds among polymers that are difficult in the usual QM calculation due to the numerical instability of the calculation and the large scales of the systems, and the second is the CCT can easily parallelize the QM calculation to reduce the calculation cost dramatically as we can finish a calculation in a realistic time span, a few days. As demonstrated in this study, the explicit consideration of the interactions among polymer chains critically influences the fine spectral features in the low-frequency region, especially the polarization directions. Not only the intermolecular interactions but also the anharmonicity of THz vibrational modes have to be considered in the future calculation studies.

CONCLUSIONS

We have studied vibrational bands of crystalline PHB in the THz region and successfully assign the intermolecular vibrational bands due to CH_3 and O═C groups appearing in both of the experimental low-frequency Raman and THz (FIR) absorption spectra. The CCT method can provide realistic spectra of the PHB with the explicit corrections for the intermolecular interactions among polymer chains, which has been desired in the simulations of the THz bands. The spectral shapes and the polarization states of the THz bands are critically influenced by the intermolecular interactions. We could confirm the existence of the weak hydrogen bonds among polymer chains along the *a* axis of PHB. This directional weak interaction among polymer chains can determine the folding direction of the crystalline PHB as proposed before.[26] Our strategy combining the Raman and FIR spectroscopies with the quantum mechanical calculations aided with the CCT method is a promising way to assign the modes in the THz region of polymers and explore their roots. This combination method should provide new insight into hydrogen bonds in various polymers and other molecules including proteins.

ASSOCIATED CONTENT

Supporting Information

Computational details. This material is available free of charge via the Internet at http://pubs.acs.org.

AUTHOR INFORMATION

Corresponding Author

*E-mail: aporoa@gmail.com (S.Y.); ozaki@kwansei.ac.jp (Y.O.).

Notes

The authors declare no competing financial interest.

ACKNOWLEDGMENTS

This work was supported by Industry-Academia Collaborative R&D from Japan Science and Technology Agency, JST, and by the JSPS research fellowship to S.Y.

REFERENCES

(1) Giraud, G.; Karolin, J.; Wynne, K. *Biophys. J.* **2003**, *85*, 1903−1913.
(2) Colaianni, S. E. M.; Nielsen, O. F. *J. Mol. Struct.* **1995**, *347*, 267−284.
(3) Renugopalakrishnan, V.; Collette, T. W.; Carreira, L. A.; Bhatnagar, R. S. *Macromolecules* **1985**, *18*, 1786−1788.
(4) Genzel, L.; Keilmann, F.; Martin, T. P.; Winterling, G.; Yacoby, Y.; Frohlich, H.; Makinen, M. W. *Biopolymers* **1976**, *15*, 219−225.
(5) Brown, K. G.; Erfurth, S. C.; E.W., S.; Peticolas, W. L. *Proc. Natl. Acad. Sci. U.S.A.* **1972**, *69*, 1467−1469.
(6) Kato, T.; Shirota, H. *J. Chem. Phys.* **2011**, *134*, 164504.
(7) Palombo, F.; Paolantoni, M.; Sassi, P.; Morresi, A.; Giorgini, M. G. *Phys. Chem. Chem. Phys.* **2011**, *13*, 16197−16207.
(8) Kapitán, J.; Dračínský, M.; Kaminský, J.; Benda, L.; Bouř, P. *J. Phys. Chem. B* **2010**, *114*, 3574−3582.
(9) Paolantoni, M.; Sassi, P.; Morresi, A.; Santini, S. *J. Chem. Phys.* **2007**, *127*, 024504.
(10) Eaves, J. D.; Fecko, C. J.; Stevens, A. L.; Peng, P.; Tokmakoff, A. *Chem. Phys. Lett.* **2003**, *376*, 20−25.
(11) Soutzidou, M.; Glezakou, V. A.; Viras, K.; Helliwell, M.; Maters, A. J.; Vincent, M. A. *J. Phys. Chem. B* **2002**, *106*, 4405−4411.
(12) Egashira, K.; Nishi, N. *J. Phys. Chem. B* **1998**, *102*, 4054−4057.
(13) Mizoguchi, K.; Hori, Y.; Tominaga, Y. *J. Chem. Phys.* **1992**, *97*, 1961−1968.
(14) Krimm, S. *Fortschr. Hochpolym. Forsch.* **1960**, *2*, 51−172.
(15) Tasumi, M.; Krimm, S. *J. Chem. Phys.* **1967**, *46*, 755.
(16) Bershtein, V. A.; Ryzhov, V. A. *Adv. Polym. Sci.* **1994**, *114*, 43−121.
(17) Shen, D. Y.; Pollack, S. K.; Hsu, S. L. *Macromolecules* **1989**, *22*, 2564−2569.
(18) Möller, K. D.; Rothschild, W. G. *Far-Infrared Spectroscopy*; Wiley-Interscience: New York, 1971.
(19) Frank, W. F. X.; Fielder, H. *Infrared Phys.* **1979**, *19*, 481−489.
(20) Herrmann, C.; Ruud, K.; Reiher, M. *ChemPhysChem* **2006**, *7*, 2189−2196.
(21) Fuse, N.; Sato, R.; Mizuno, M.; Fukunaga, K.; Itoh, K.; Ohki, Y. *Jpn. J. Appl. Phys.* **2010**, *49*, 102402.
(22) Satkowski, M. M.; Melik, D. H.; Autran, J. P.; Green, P. R.; Nosa, I.; Schechtman, L. A. *Physical and Processing Properties of Polyhydroxyalkanoate (PHA) Copolymers*; Wiley-VCH: Weinheim, Germany, 2001.
(23) Holmes, P. A. *Biologically Produced (R)-3-Hydroxyalkanoate Polymers and Copolymers*; Elsevier: London, 1988; Vol. 2.
(24) Yokouchi, M.; Chatani, Y.; Tadokoro, H.; Teranishi, K.; Tani, H. *Polymer* **1973**, *14*, 267−272.
(25) Iwata, T.; Aoyagi, Y.; Tanaka, T.; Fujita, M.; Takeuchi, A.; Suzuki, Y.; Uesugi, K. *Macromolecules* **2006**, *39*, 5789−5795.
(26) Sato, H.; Ando, Y.; Dybal, J.; Iwata, T.; Noda, I.; Ozaki, Y. *Macromolecules* **2008**, *41*, 4305−4312.
(27) Sato, H.; Mori, K.; Murakami, R.; Ando, Y.; Takahashi, I.; Zhang, J.; Terauchi, H.; Hirose, F.; Senda, K.; Tashiro, K.; Noda, I.; Ozaki, Y. *Macromolecules* **2006**, *39*, 1525−1531.
(28) Sato, H.; Dybal, J.; Murakami, R.; Noda, I.; Ozaki, Y. *J. Mol. Struct.* **2005**, *744*−*747*, 35−46.
(29) Sato, H.; Nakamura, M.; Padermshoke, A.; Yamaguchi, H.; Terauchi, H.; Ekgasit, S.; Noda, I.; Ozaki, Y. *Macromolecules* **2004**, *37*, 3763−3769.
(30) Sato, H.; Murakami, R.; Padermshoke, A.; Hirose, F.; Senda, K.; Noda, I.; Ozaki, Y. *Macromolecules* **2004**, *37*, 7203−7213.
(31) Matsuura, H.; Yoshida, H.; Hieda, M.; Yamanaka, S.; Harada, T.; Shin-ya, K.; Ohno, K. *J. Am. Chem. Soc.* **2003**, *125*, 13910−13911.
(32) Harada, T.; Yoshida, H.; Ohno, K.; Matsuura, H. *Chem. Phys. Lett.* **2002**, *362*, 453−460.
(33) Woo, S.; Kim, K. *J. Phys. Chem.* **1996**, *100*, 17124−17132.
(34) Sander, W.; Gantenberg, M. *Spectrochim. Acta A* **2005**, *62*, 902−909.
(35) Hoshina, H.; Morisawa, Y.; Sato, H.; Kamiya, A.; Noda, I.; Ozaki, Y.; Otani, C. *Appl. Phys. Lett.* **2010**, *100*, 101904.
(36) Hoshina, H.; Morisawa, Y.; Sato, H.; Minamide, H.; Noda, I.; Ozaki, Y.; Otani, C. *Phys. Chem. Chem. Phys.* **2011**, *13*, 9173−9179.
(37) Wietzke, S.; Jansen, C.; Jung, T.; Reuter, M.; Baudrit, B.; Bastian, M.; Chatterjee, S.; Koch, M. *Opt. Express* **2009**, *17*, 19006−19014.
(38) Kambara, O.; Tamura, A.; Uchino, T.; Yamamoto, K.; Tominaga, K. *Biopolymers* **2010**, *93*, 735−739.

(39) Wietzke, S.; Jansen, C.; Reuter, M.; Jung, T.; Hehl, J.; Kraft, D.; Chatterjee, S.; Greiner, A.; Koch, M. *Appl. Phys. Lett.* **2010**, *97*, 022901.
(40) Bouř, P.; Keiderling, T. A. *J. Chem. Phys.* **2002**, *117*, 4126−4132.
(41) Bouř, P.; Sopková, J.; Bednárová, L.; Maloň, P.; Keiderling, T. A. *J. Comput. Chem.* **1997**, *18*, 646−659.
(42) Yamamoto, S.; Li, X.; Ruud, K.; Bouř, P. *J. Chem. Theory Comput.* **2012**, *8*, 977−985.
(43) Andrushchenko, V.; Bouř, P. *Chirality* **2010**, *22*, E96−E114.
(44) Yamamoto, S.; Kaminský, J.; Bouř, P. *Anal. Chem.* **2012**, *84*, 2440−2451.
(45) Kubelka, J.; Keiderling, T. A. *J. Am. Chem. Soc.* **2001**, *123*, 12048−12058.
(46) Yamamoto, S.; Watarai, H.; Bouř, P. *Chem. Phys. Chem.* **2011**, *12*, 1509−1518.
(47) Hudecová, J.; Kapitán, J.; Baumruk, V.; Hammer, R. P.; Keiderling, T. A.; Bouř, P. *J. Phys. Chem. A* **2010**, *114*, 7642−7651.
(48) Yamamoto, S.; Straka, M.; Watarai, H.; Bouř, P. *Phys. Chem. Chem. Phys.* **2010**, *12*, 11021−11032.
(49) Profant, V.; Baumruk, V.; Li, X.; Šafařík, M.; Bouř, P. *J. Phys. Chem. B* **2011**, *115*, 15079−15089.
(50) Andrushchenko, V.; Bouř, P. *J. Phys. Chem. A* **2007**, *111*, 9714−9723.
(51) Andrushchenko, V.; Wieser, H.; Bouř, P. *J. Phys. Chem. B* **2002**, *106*, 12623−12634.
(52) Andrushchenko, V.; Tsankov, D.; Krasteva, M.; Wieser, H.; Bouř, P. *J. Am. Chem. Soc.* **2011**, *133*, 15055−15064.
(53) Bouř, P. *Collect. Czech. Chem. Commun.* **2005**, *70*, 1315−1340.
(54) Papanek, P.; Fischer, J. E.; Murthy, N. S. *Macromolecules* **2002**, *35*, 4175−4182.
(55) Bouř, P. Academy of Sciences, Prague, Czech Republic, 2002−2006.
(56) Frisch, M. J.; Trucks, G. W.; Schlegel, H. B.; Scuseria, G. E.; Robb, M. A.; Cheeseman, J. R.; Scalmani, G.; Barone, V.; Mennucci, B.; Petersson, G. A.; Nakatsuji, H.; Caricato, M.; Li, X.; Hratchian, H. P.; Izmaylov, A. F.; Bloino, J.; Zheng, G.; Sonnenberg, J. L.; Hada, M.; Ehara, M.; Toyota, K.; Fukuda, R.; Hasegawa, J.; Ishida, M.; Nakajima, T.; Honda, Y.; Kitao, O.; Nakai, H.; Vreven, T.; Montgomery, J., J. A.; Peralta, J. E.; Ogliaro, F.; Bearpark, M.; Heyd, J. J.; Brothers, E.; Kudin, K. N.; Staroverov, V. N.; Kobayashi, R.; Normand, J.; Raghavachari, K.; Rendell, A.; Burant, J. C.; Iyengar, S. S.; Tomasi, J.; Cossi, M.; Rega, N.; Millam, N. J.; Klene, M.; Knox, J. E.; Cross, J. B.; Bakken, V.; Adamo, C.; Jaramillo, J.; Gomperts, R.; Stratmann, R. E.; Yazyev, O.; Austin, A. J.; Cammi, R.; Pomelli, C.; Ochterski, J. W.; Martin, R. L.; Morokuma, K.; Zakrzewski, V. G.; Voth, G. A.; Salvador, P.; Dannenberg, J. J.; Dapprich, S.; Daniels, A. D.; Farkas, Ö.; Foresman, J. B.; Ortiz, J. V.; Cioslowski, J.; Fox, D. J. *Gaussian09*; Gaussian, Inc.: Wallingford, CT, 2009.
(57) Hamprecht, F. A.; Cohen, A. J.; Tozer, D. J.; Handy, N. C. *J. Chem. Phys.* **1998**, *109*, 6264−6271.
(58) Rao, L.; Ke, H.; Fu, G.; Xu, X.; Yan, Y. *J. Chem. Theor. Comput.* **2009**, *5*, 86−96.
(59) Bouř, P. Academy of Sciences, Prague, Czech Republic.
(60) Abe, H.; Doi, Y.; Aoki, H.; Akehata, T. *Biopolymers* **1998**, *31*, 1791−1797.
(61) Becke, A. D. *J. Chem. Phys.* **1993**, *98*, 5648−5652.
(62) Perdew, J. P.; Burke, K.; Wang, Y. *Phys. Rev. B* **1996**, *54*, 16533−16539.
(63) Xu, X.; Goddard, W. A. I. *Proc. Natl. Acad. Sci. U.S.A.* **2004**, *101*, 2673−2677.
(64) Grimme, S. *J. Comput. Chem.* **2006**, *27*, 1787−1799.
(65) Yanai, T.; Tew, D. P.; Handy, N. C. *Chem. Phys. Lett.* **2004**, *393*, 51−57.